ORIGINAL ARTICLE
Iran J Allergy Asthma Immunol
August 2024; 23(4):437-451.
DOI: 10.18502/ijaai.v23i4.16217

Synergistic Treatment Approach for Pulmonary Fibrosis: Prednisone and Cyclophosphamide Regulation of Circular RNA MORF4L1 and MicroRNA-29a-3p Targeting *BRD4*

Dan Wang[1], Hao Zhao[2], Ben Li[1], and Feng Quan[1]

[1] Department of Rheumatology, Yueyang Hospital of Integrated Traditional Chinese and Western Medicine, Shanghai University of Traditional Chinese Medicine, Shanghai, China
[2] Department of Emergency, Shanghai TCM – Integrated Hospital, Shanghai University of Traditional Chinese Medicine, Shanghai, China

Received: 24 April 2024; Received in revised form: 15 July 2024; Accepted: 18 July 2024

ABSTRACT

This study aimed to explore the effect of prednisone (PDN) combined with cyclophosphamide (CTX) on bleomycin-induced pulmonary fibrosis (PF) in rats via circular RNA mortality factor 4 like 1 (MORF4L1)/microRNA (miR)-29a-3p/Bromodomain protein 4 (BRD4) axis.

A rat model of PF was induced by bleomycin and treated with PDN combined with CTX, and the lentiviral vectors that interfered with MORF4L1, miR-29a-3p, or *BRD4* expression were injected into the tail vein at the same time. The mRNA expressions of MORF4L1, miR-29a-3p, BRD4, and fibrosis-associated proteins including fibronectin, connective tissue growth factor, and collagen I were detected by real-time quantitative polymerase chain reaction. The expression level of BRD4 protein in rat lungs was detected by Western blot analysis. Lung pathology of rats was observed by hematoxylin and eosin and Masson's trichrome staining. Apoptosis was observed by terminal deoxynucleotidyl transferase dUTP nick end labeling staining. The targeting relationship between miR-29a-3p and MORF4L1 or BRD4 was verified by the bioinformatics website and dual luciferase reporter experiment.

Bleomycin-induced PF enhanced MORF4L1 and BRD4 expression, inhibited miR-29a-3p expression, injured lung tissue, increased mRNA expression of fibrosis-related markers, and induced apoptosis in the lung tissue of rats. PDN combined with CTX had a therapeutic effect on PF in rats, which was further promoted by down-regulating MORF4L1 or up-regulating miR-29a-3p. After down-regulating miR-29a-3p or up-regulating BRD4, the effect of down-regulating MORF4L1 was reversed. MORF4L1 could bind to miR-29a-3p to target BRD4.

In short, PDN combined with CTX can effectively improve PF through downregulating MORF4L1 to enhance miR-29a-3p-targeted regulation of BRD4.

Keywords: Bromodomain protein 4; Circular RNA mortality factor 4 like 1; Cyclophosphamide; MicroRNA-29a-3p; Prednisone; Pulmonary fibrosis

Corresponding Author: Hao Zhao, MD;
Department of Emergency, Shanghai TCM‐Integrated Hospital, Shanghai University of Traditional Chinese Medicine, Shanghai, China. Email: zhaohappy@hotmail.com

INTRODUCTION

Pulmonary fibrosis (PF) is a disease induced by interstitial pneumonia; however, to the best of our

Copyright © 2024 Wang et al. Published by Tehran University of Medical Sciences.

This work is licensed under a Creative Commons Attribution-NonCommercial 4.0 International license (https://creativecommons.org/licenses/by-nc/4.0/). Non-commercial uses of the work are permitted, provided the original work is properly cited.

knowledge, the mechanism underlying the occurrence of this disease is yet to be elucidated.[1,2] At present, injury to epithelial cells, cellular senescence, and an abnormal immune response are considered to contribute to lung fibrosis development.[3-5] Moreover, the excessive accumulation of fibroblasts and the increased secretion of extracellular matrix promotes the fibrosis of lung tissues.[6] PF can be categorized into immune, primary, drug-induced, and idiopathic types, based on its pathogenesis.[7] Idiopathic pulmonary fibrosis (IPF), a chronic and progressive fibrotic lung disease, is a well-recognized form of idiopathic interstitial pneumonia. The clinical presentation encompasses pulmonary dysfunction and a gradual onset of dyspnea. The pathological process involves the destruction of alveolar architecture and excessive accumulation of extracellular matrix, leading to compromised gas exchange and reduced lung compliance. Ultimately, these changes culminate in respiratory failure and mortality. The incidence and mortality rates of IPF exhibit an upward trend, primarily among individuals in the middle-aged and elderly demographic (55 to 75 years old). The median survival duration for patients diagnosed with IPF is notably brief, typically ranging from 3 to 5 years.[8,9] Risk factors linked to IPF consist of smoking history, age, occupational exposure, genetic changes, and viral infection.[10,11]

Several pharmaceutical agents, namely acetylcysteine, pirfenidone, and prednisone, have been identified as viable treatment options for PF.[12-14] At present, two regimens for PF treatment are prednisone (PDN) with cyclophosphamide (CTX) or azathioprine.[13-15] However, the investigation into the precise mechanisms by which drugs exert their effects on subsequent processes is infrequently undertaken.

Circular RNAs (circRNAs) are noncoding RNAs that are produced by reverse splicing of introns or exons, resulting in the formation of a covalently closed loop structure.[16,17] In recent decades, a growing body of evidence has demonstrated the pivotal role of circRNAs in the etiology and progression of diverse diseases, including cardiovascular disease, cancer, and diabetes.[18-20] circRNAs are commonly recognized as molecules that function as microRNA (miR) sponges, thereby competitively binding to their target genes. This interaction leads to alterations in signal transductions and disruptions in gene expression.[21] Studies have provided comprehensive insights into the significant involvement of the circRNA/miR/mRNA axis in various disease pathogenesis and developmental pathways.[22-24] *MORF4L1* is upregulated in pneumonia and accelerates apoptosis of epithelial cells,[25] but its role in PF is rarely studied.

MicroRNAs are closely implicated in PF.[26-28] miR-29 has been reported to be significantly reduced in some fibrotic diseases associated with the lung, heart, and liver.[29,30] Moreover, miR-29a-3p can suppress the activation of lung fibroblast.[31] miR-29a-3p expression is decreased in both in vitro and in vivo PF models.[32] Bromodomain protein 4 (*BRD4*) is elevated in PF, and depression of *BRD4* can alleviate PF.[33,34] In this study, we proposed for the first time that PDN combined with CTX could improve PF by regulating *MORF4L1*/miR-29a-3p/*BRD4* axis and explored the specific mechanism.

MATERIALS AND METHODS

Experimental Animals

Healthy Wistar rats weighing 200 to 250 g (SLAC Laboratory Animals Co., Ltd, Shanghai, China) were acclimated to the laboratory environment for 7 days in a temperature-controlled room maintained at (23±2)°C, with suitable humidity and a 12-hour light-dark cycle. The rats were fed standard food and water. The study was implemented in strict accordance with the recommendations in the National Institutes of Health guidelines for the care and use of laboratory animals. All experimental protocols were approved by the Ethics Committee of Yueyang Hospital of Integrated Traditional Chinese and Western Medicine, Shanghai University of Traditional Chinese Medicine (Approval Number: 2019YYZ06). All operations were performed under pentobarbital sodium (50 mg/kg) anesthesia to minimize pain.

PF Model Establishment

A 0.2-mL injection of bleomycin (BLM) at a dosage of 5 mg/kg, obtained from Aladdin (B107423, China), was administered into the trachea of rats to induce PF. The control group of rats received an equivalent volume of saline injection.[35]

Grouping and Treatment

Rats were medicated 48 hours after modeling. sh-*MORF4L1*, miR-29a-3p agomir, miR-29a-3p antagomir, overexpressed *BRD4* (oe-*BRD4*), and their negative controls (NC) (sh-NC, agomir NC, antagomir NC, and oe-NC) lentiviral vectors were obtained from GenePharma (Shanghai, China). The virus titers were measured at a concentration of 108 transduction units (TU)/mL. Six rats in the control group were selected as the sham group, and 60 successfully modeled rats were randomly divided into 12 groups (n=6). In the following groups, the rats were intraperitoneally injected with 5 mL of normal saline or a corresponding mixed solution. (1) model group (saline injection); (2) PDN group (injection with 5 mg/kg PDN); (3) CTX group (injection with 15mg/kg CTX); (4) combined intervention group

(PDN+ CTX) (injection with 5mg/kg PDN and 15 mg/kg CTX). In the following groups, after the intervention, the rats were injected with corresponding lentivirus vector through the tail vein: (5) sh-*MORF4L1* group (PDN+ CTX+ sh-*MORF4L1*); (6) sh-NC group (PDN+ CTX+ sh-NC); (7) miR-29a-3p agomir group (PDN+ CTX+ miR-29a-3p agomir); (8) agomir NC group (PDN+ CTX+ agomir NC); (9) sh-*MORF4L1*+ antagomir NC group (PDN+ CTX+ sh-*MORF4L1*+ antagomir NC); (10) sh-*MORF4L1*+ miR-29a-3p antagomir group (PDN+ CTX+ sh-*MORF4L1*+ miR-29a-3p antagomir); (11) sh-*MORF4L1*+ oe-*BRD4* group (PDN+ CTX+ sh-*MORF4L1*+ oe-*BRD4*); (12) sh-*MORF4L1*+ oe-NC group (PDN+ CTX+ sh-*MORF4L1*+ oe-NC). After 28 days, the rats were euthanized by inhalation of 5% isoflurane (HR135327; Hairui Chemical, Shandong, China) for 30 seconds prior to cervical dislocation, as previously described.[36,37] The death of rats was verified by the lack of heartbeat and a cold body. Plasma and lung tissue samples were then collected.

Enzyme-linked Immunosorbent Assay (ELISA)

The levels of inflammatory factors including tumor necrosis factor-α (TNF-α), interleukin (IL)-1β, and IL-6 in rat plasma were detected. ELISA kits utilized included mouse TNF-α (EK0527; sensitivity, 2.0 pg/mL), mouse IL-1β (EK0394; sensitivity, 3.8 pg/mL), and mouse IL-6 (EK0411; sensitivity, 5.0 pg/mL) (Boster, Wuhan, China).

Sample Collection

Sections of the lung were excised and subjected to fixation in neutral formalin, dehydration, embedding, sectioning, routine hematoxylin and eosin (H&E), and Masson staining. The remaining portions were submerged in liquid nitrogen and preserved at −80℃.

Paraffin Sections

The lung tissue underwent a series of procedures including fixation in 10% methanol, dehydration, clearance, wax immersion, and embedding, resulting in tissue wax blocks. The tissue was sliced into 5-μm sections and subsequently flattened using a constant temperature spread sheet baking machine. Following complete stretching, the sections were affixed onto the slide that had been coated with polylysine, and subsequently subjected to baking in an oven at 60℃.

Hematoxylin and Eosin Staining

The paraffin sections underwent a series of procedures including dewaxing, immersion in xylene and anhydrous ethanol, staining with hematoxylin, and washing with Tris-buffered saline with Tween 20 (TBST) and eosin. Subsequently, dehydration, clearance, sealing, and sequential alcohol dehydration and xylene clearance were performed. Following drying, the sections were sealed with neutral gum and preserved. To evaluate the histopathological changes in the lungs, TCS SP8 laser scanning confocal microscopy was utilized to examine 10 randomly selected high-magnification (400×) regions in each sample.

Masson Staining

Paraffin sections were routinely dewaxed (similar to H&E staining), treated with Boain solution, stained with hematoxylin, differentiated by hydrochloric acid and alcohol, and soaked in ammonia. Sections were treated with ponceau and 1% molybdate phosphomolybdic acid solution and then counter-stained with aniline blue solution. The aniline blue was washed off with 95% ethanol and then 100% anhydrous ethanol. After xylene clearance, the sections were sealed with neutral gum and evaluated by Ashcroft score. Ten regions with high magnification (400×) were randomly selected in each specimen. The average scores of these regions were utilized as fibrosis scores for the sample.

TdT-mediated dUTP-biotin Nick End-labeling (TUNEL) Staining

Apoptosis in the lung tissue was detected by Cell Death Detection Kit (Roche, Mannheim, Germany). Shortly, 4% paraformaldehyde-fixed lung tissue was blocked with 3% H_2O_2, treated with fluorescein isothiocyanate-dUTP (green) and 4,6-diamino-2-phenylindole (blue), and imaged under a fluorescence microscope (Olympus, Tokyo, Japan). Apoptosis rate was defined as the percentage of TUNEL-positive cells/total cells.

Real-time Fluorescence Quantitative Polymerase Chain Reaction

Total RNA was extracted from rat lung tissue with Trizol (Invitrogen, Carlsbad, CA, USA) and reversely transcribed into cDNA using a cDNA synthesis kit (Fermentas Inc., Ontario, CA, USA). RT-qPCR was by StepOnePlus Real-Time PCR system (Applied Biosystems Inc.). The reaction conditions were as follows: predenaturation at 95°C for 10 minutes, 40 cycles of denaturation at 95°C for 15 seconds, and annealing at 60°C for 1 minute. PCR primers were designed and synthesized by Invitrogen (supplementary Table 1). U6 was the internal reference for miR-29a-3p, and glyceraldehyde 3-phosphate dehydrogenase (GAPDH) was that for *MORF4L1*, *BRD4*, *CTGF*, collagen I, and *FN*. The amplified product was verified by agarose gel electrophoresis. The data were analyzed by the $2^{-\Delta\Delta Ct}$ method.

Published by Tehran University of Medical Sciences (http://ijaai.tums.ac.ir)

Western Blot Detection

Total protein was extracted in line with a bicinchoninic acid kit (BOSTER Biological Technology Co. Ltd., Wuhan, China), and protein concentration was determined. The proteins were then isolated by 10% polyacrylamide gel electrophoresis and electro-imprinted onto the polyvinylidene fluoride membrane. The membrane was blocked with 5% bovine serum albumin, followed by incubation with primary antibody *BRD4* (1: 1000) (Abcam, UK) and corresponding secondary antibody (MT-BIO, Shanghai, China). GAPDH (1: 1000; Cell Signaling Technology) was regarded as an internal reference. Finally, the membrane was imaged by Bio-Rad Gel Doc EZ IMAGER (Bio-Rad, California, USA). ImageJ software was employed to analyze the gray value of the target band.

The luciferase Report Experiment

Bioinformatics website predicted *MORF4L1*, miR-29a-3p, and *BRD4*'s targeting relations and binding sites. GenePharma was commissioned to construct the *MORF4L1*-3′ untranslated region (UTR) wild-type (WT) (*MORF4L1*-WT) and mutant (MUT) plasmids (*MORF4L1*-MUT), and *BRD4*-WT and -MUT. Rat lung epithelial cells L2, which were logarithmically grown and obtained from the Stem Cell Bank of the Chinese Academy of Sciences, were plated into 96-well plates. Upon reaching 70% cell confluence, Lipofectamine 2000 (Invitrogen) was cotransfected into L2 cells along with plasmids containing miR-29a-3p mimic and its NC. Subsequently, luciferase activity was measured using a luciferase assay kit (BioVision, San Francisco, CA, USA).

Statistical Analysis

SPSS 21.0 (SPSS Inc, Chicago, IL, USA) statistical software was applied for the analysis of data, and measurement data were expressed as mean±standard deviation (SD). The *t* test was employed to compare the measurement data of 2 groups that followed a normal distribution, while one-way analysis of variance (ANOVA) was utilized to compare multiple groups. Pair comparisons were conducted using the least significant difference method (LSD method). *p* was a bilateral test, and $p<0.05$ was considered statistically significant.

RESULTS

PDN Combined with CTX Inhibits Levels of Fibrosis-related Markers and Improves PF

PF was induced through endotracheal injection of BLM in rats, and then intraperitoneal injection of PDN or CTX was implemented. The pathology in lung tissue was observed, finding that there was inflammatory cell infiltration, collagen deposition, and diffuse and dense fibrosis in the model group. Pathology was alleviated in the PDN, CTX, or combined intervention groups, with the combined intervention group showing the best treatment effect (Figures 1A and 1B). ELISA results showed that the content of inflammatory factors (TNF-α, IL-1β, and IL-6) was increased in PF rats, which could be reduced when PDN or CTX was administrated. The best effect was obtained after combined treatment (Supplementary Figures 1A-C). These results proved that the PF rat model was successfully established, and PDN and CTX had therapeutic effects on PF rats. Then we measured the mRNA expressions of fibrosis-related markers *CTGF*, collagen I, and *FN* by RT-qPCR. The expression of fibrosis-related markers in rats with PF was observed to be elevated, but this increase was mitigated following the administration of either PDN or CTX individually or in combination. TUNEL staining found that PF induced apoptosis in the lung tissue of rats, and treatment with PDN or CTX could attenuate this phenomenon. The combination of PDN and CTX demonstrated a significant decrease in apoptosis rate (Figure 1F). In the model group, the expression levels of *MORF4L1* and *BRD4* were observed to be upregulated, while miR-29a-3p was found to be downregulated. Conversely, in the PDN, CTX, or combined intervention groups, the trends were reversed, with the combined intervention group exhibiting the most significant alterations (Figures 1G to 1I). Briefly, PDN or CTX improves PF, and the combined application of the 2 is the most effective. Therefore, PDN and CTX were selected for subsequent experiments.

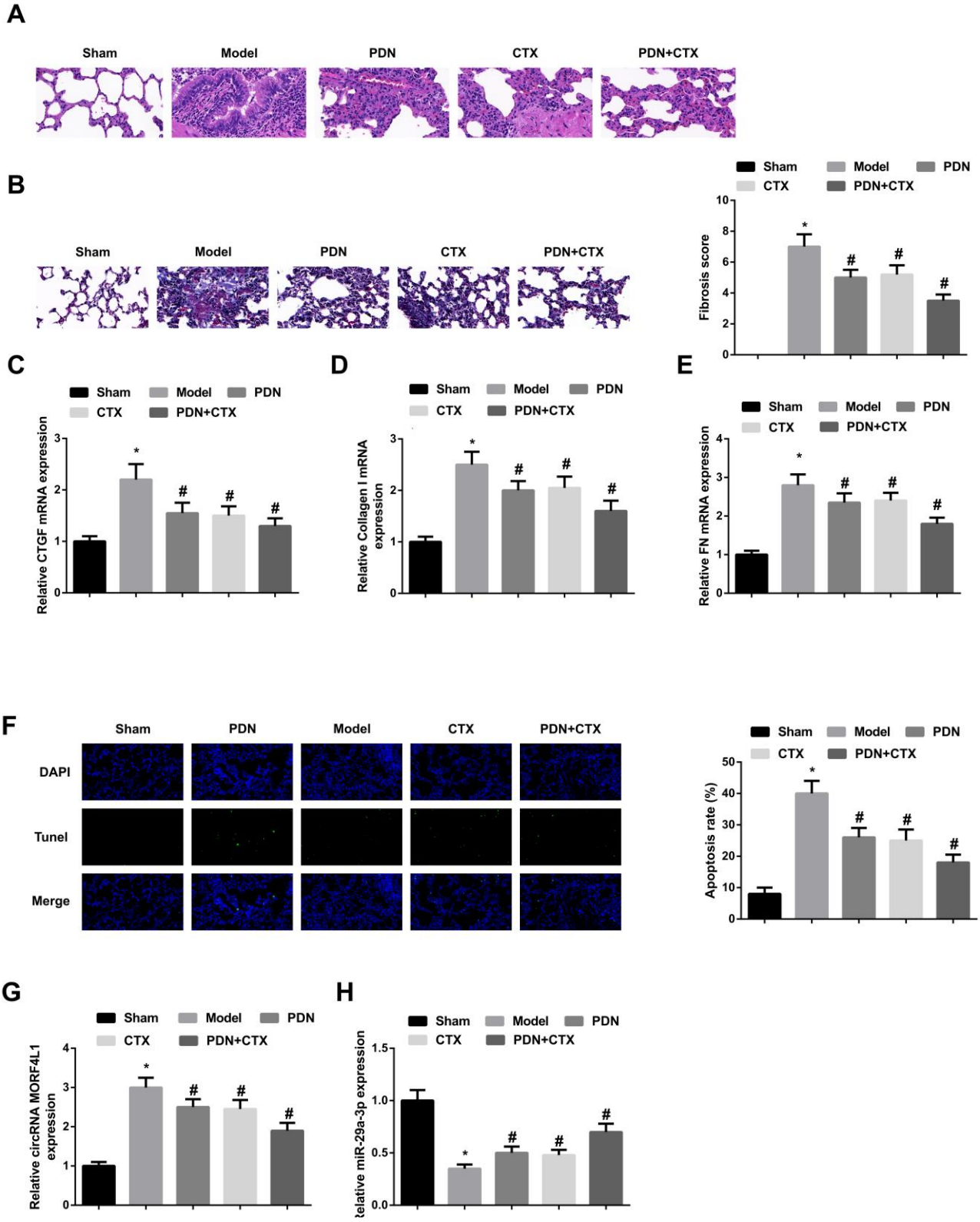

Published by Tehran University of Medical Sciences (http://ijaai.tums.ac.ir)

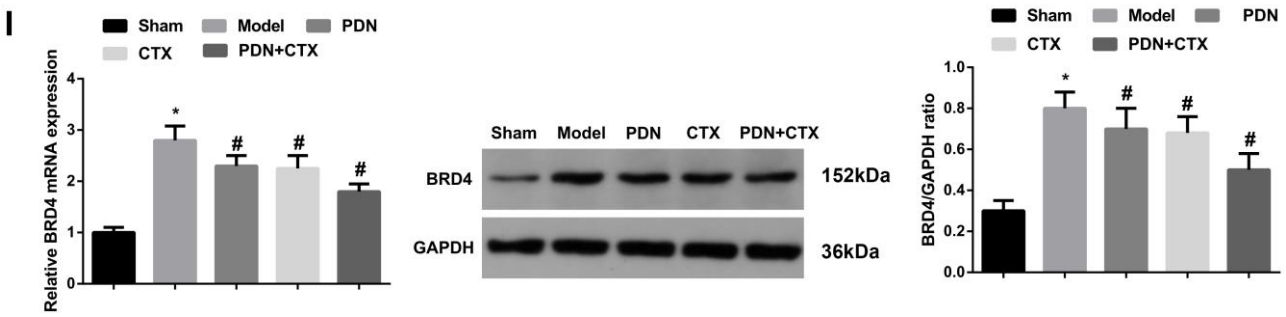

Figure 1. Prednisone (PDN) combined with cyclophosphamide (CTX) inhibits levels of fibrosis-related markers and improves pulmonary fibrosis (PF). A. hematoxylin and eosin (HE) staining (400×) showed that the Model group had inflammatory cell infiltration and pathological conditions were improved in the PDN group, CTX group, or combined intervention group, among which the combined intervention group had the best therapeutic effect; B. Masson staining (400×) showed that collagen fibers in the Model group increased significantly, with diffuse and dense fibrosis. Pathological conditions of the PDN group, CTX group, or combined intervention group were improved, among which the combined intervention group had the best treatment effect; C/D/E. real-time quantitative polymerase chain reaction (RT-qPCR) showed that the expression level of fibrosis-related markers increased in the Model group, while decreased in the PDN, CTX, or combined intervention groups, with the highest decrease in the combined intervention group; F. terminal deoxynucleotidyl transferase dUTP nick end labeling (TUNEL) staining (400×) found that the apoptosis of lung tissue cells increased in the Model group, and decreased in the PDN group, CTX group or combined intervention group, among which the combined intervention group had the best therapeutic effect; G/H/I. mortality factor 4 like 1 (*MORF4L1),* miR-29a-3p, and bromodomain-containing protein 4 (*BRD4)* detected by RT-qPCR and Western Blot; The values were represented as mean±SD, n=6, * p<0.05 vs Sham; # p<0.05 vs Model.

Downregulated *MORF4L1* Can Further Alleviate PF

After PDN + CTX intervention, sh-*MORF4L1* and sh-NC were injected through the caudal vein, respectively. The successful injection was verified by RT-qPCR (Figure 2A). HE and Masson staining were used to observe the lung tissue pathology of rats, and the results showed that the lung tissue pathology of rats was improved after *MORF4L1* downregulation (Figures 2B and 2C). The mRNA expressions of fibrosis-associated markers (CTGF, collagen I, and FN) were detected by RT-qPCR. The results showed that expression levels of fibrosis-related markers decreased after *MORF4L1* was downregulated (Figures 2D to 2F). TUNEL staining was used to detect apoptosis of rat lung tissue cells, and the results showed that apoptosis of lung tissue cells decreased after *MORF4L1* was downregulated (Figure 2G). Shortly, downregulating *MORF4L1* could further mitigatee PF.

***MORF4L1* Binds with miR-29a-3p**

Bioinformatics website starBase predicted the binding sites of *MORF4L1* with miR-29a-3p (Figure 3A). The luciferase reporting technique was employed to validate the interaction between *MORF4L1* and miR-29a-3p. A decrease in luciferase activity was observed subsequent to the cotransfection of *MORF4L1*-WT with miR-29a-3p mimic (Figure 3B). miR-29a-3p expression was elevated by silencing*MORF4L1* (Figure 3C).

Upregulation of miR-29a-3p Can Further Relieve PF

After PDN + CTX intervention, miR-29a-3p agomir and agomir NC were injected through the caudal vein, respectively. The successful injection was verified by RT-qPCR (Figure 4A). It was found that miR-29a-3p upregulation alleviated the pathological condition of rat lung tissue, reduced levels of CTGF, collagen I, FN, and suppressed apoptosis rate in the lung tissue (Figures 4B to 4G). Shortly, upregulating miR-29a-3p could further mitigate PF.

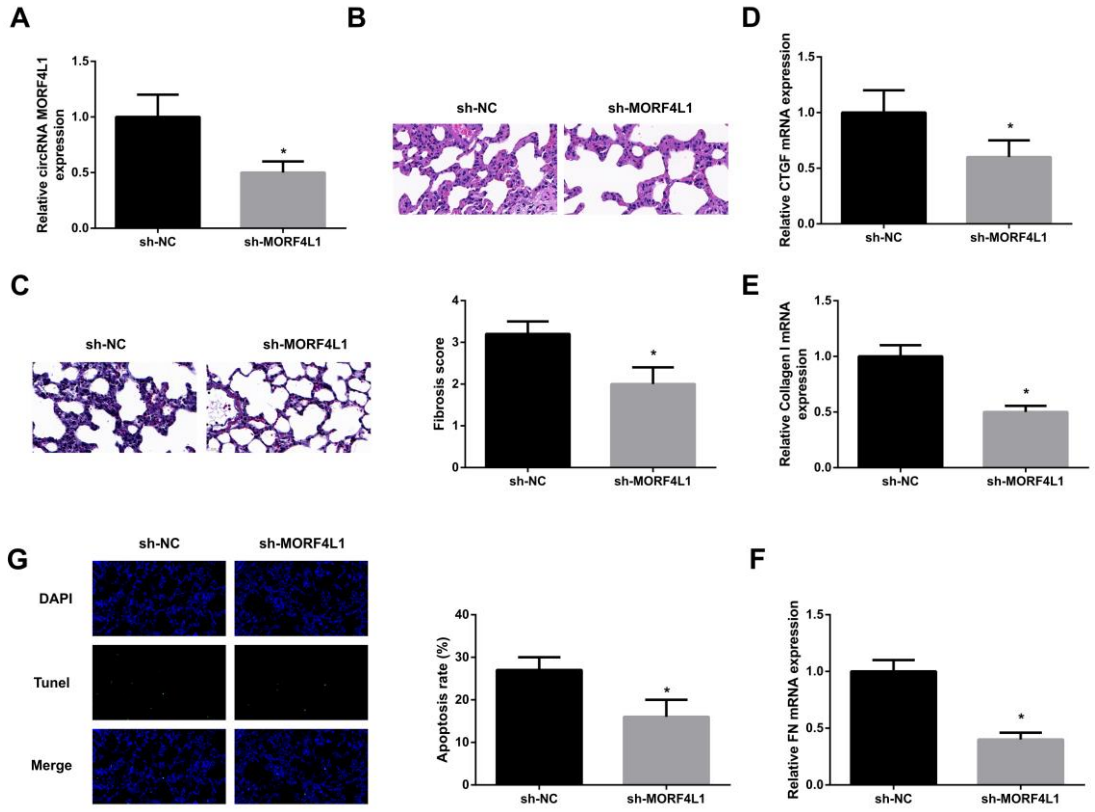

Figure 2. Repressive mortality factor 4 like 1 (*MORF4L1)* can further mitigate PF

A. *MORF4L1* detected by real-time quantitative polymerase chain reaction (RT-qPCR); B. hematoxylin and eosin (HE) staining (400×) observed lung pathology and showed that downregulated *MORF4L1* inhibited inflammatory cell infiltration; C. Masson staining (400×) observed the pathological conditions of lung tissues, and the results showed that downregulated *MORF4L1* inhibited collagen deposition; D/E/F. RT-qPCR detected fibrosis-related markers connective tissue growth factor (CTGF), collagen I, and fibronectin (FN) and found that downregulation of *MORF4L1* inhibited the expression of fibrosis-related markers; G. terminal deoxynucleotidyl transferase dUTP nick end labeling (TUNEL) staining (400×) showed that downregulating *MORF4L1* inhibited lung cell apoptosis; The values were represented as mean±SD, n=6, * p<0.05 vs short hairpin- negative control (sh-NC).

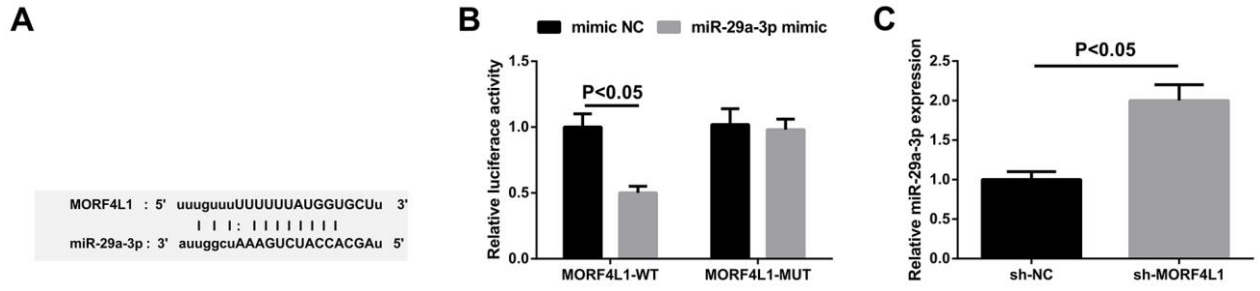

Figure 3. Mortality factor 4 like 1 (*MORF4L1)* binds to miR-29a-3p

A. The binding sites of *MORF4L1* with microRNA 29a-3p (miR-29a-3p); B. Dual luciferase reporter test verified the targeting relationship between *MORF4L1* and miR-29a-3p. The results showed that the luciferase activity decreased after *MORF4L1*-wild-type (WT) was cotransfected with miR-29a-3p mimic; C. miR-29a-3p in rat lung tissue detected by real-time quantitative polymerase chain reaction (RT-qPCR); The values were represented as mean±SD.

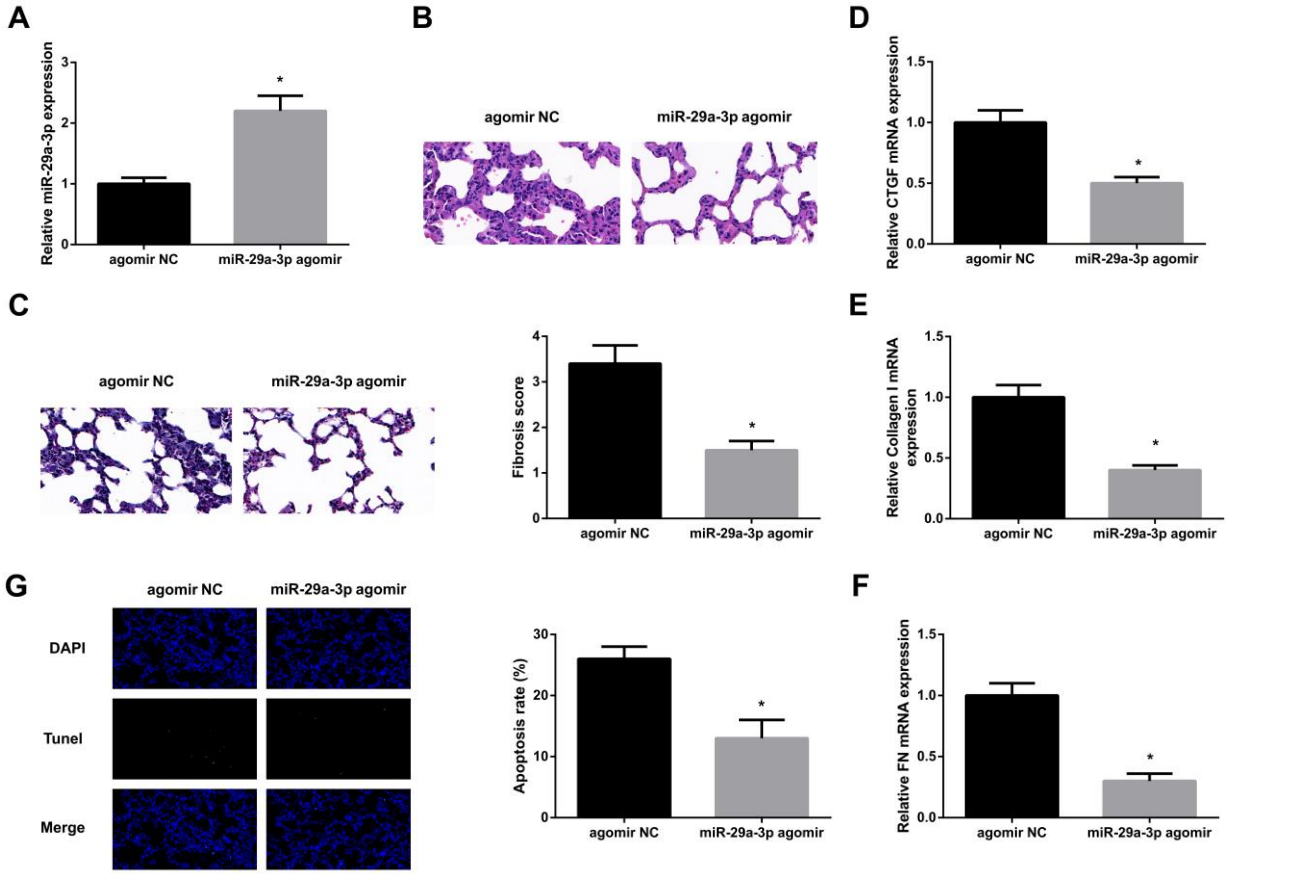

Figure 4. Augmented microRNA 29a-3p (miR-29a-3p) can further relieve PF

A. miR-29a-3p detected by real-time quantitative polymerase chain reaction (RT-qPCR); B. hematoxylin and eosin (HE) staining (400×) observed pathological condition of lung tissues observed pathological condition of lung tissues, and the results showed that upregulation of miR-29a-3p inhibited inflammatory cell infiltration; C. Masson staining (400×) observed pathological condition of lung tissues, and the results showed that upregulation of miR-29a-3p inhibited collagen deposition; D/E/F. RT-qPCR detected fibrosis-related markers connective tissue growth factor (CTGF), Collagen I, and fibronectin (FN) and found that upregulation of miR-29a-3p inhibited the expression of fibrosis-related markers; G. terminal deoxynucleotidyl transferase dUTP nick end labeling (TUNEL) staining (400×) detected apoptosis of lung tissue cells and found that upregulation of miR-29a-3p inhibited apoptosis of lung tissue cells; The values were represented as mean±SD, n=6, * p<0.05 vs agonist to microRNA (agomir) negative control (NC).

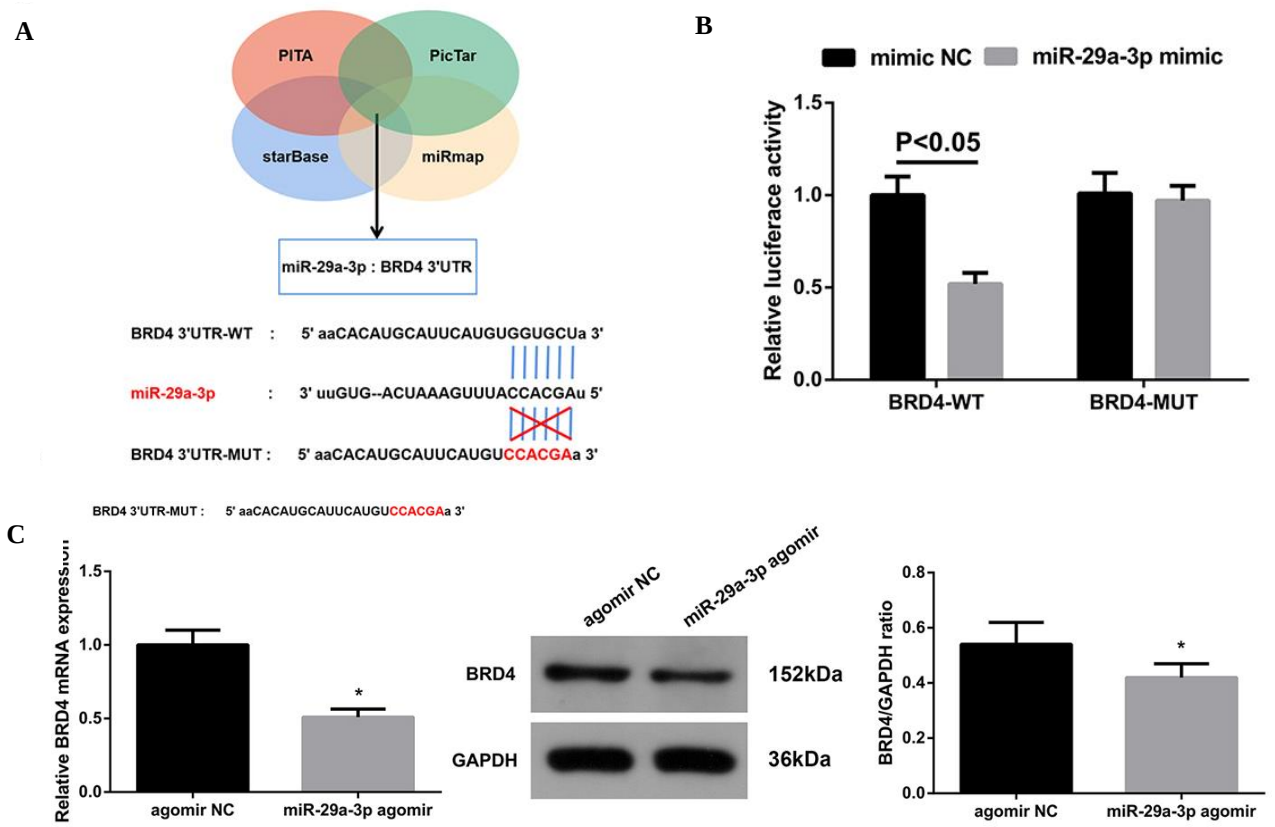

Figure 5. MicroRNA 29a-3p (miR-29a-3p) negatively regulates bromodomain-containing protein 4 (*BRD4*)
A. The binding sites of miR-29a-3p with *BRD4*; B. Dual luciferase reporter test verified the targeting relationship between miR-29a-3p and *BRD4*. The results showed that the luciferase activity decreased after cotransfection of *BRD4*- wild-type (WT) with miR-29a-3p mimic (N=3); C. *BRD4* in rat lung tissue detected via real-time quantitative polymerase chain reaction (RT-qpcr) and Western Blot (n=6); The values were represented as mean±SD. * $p<0.05$ vs agonist to microRNA (agomir) negative control (NC).

miR-29a-3p Targets *BRD4*

The gene targets *BRD4* of miR-29a-3p was cross-screened through 4 bioinformatics websites, starBase, PITA, miRmap, and PicTar (Figure 5A). The luciferase reporting technique was utilized to validate *BRD4* as the downstream target of miR-29a-3p. Luciferase activity subsequent to the cotransfection of *BRD4*-WT with the miR-29a-3p mimic was reduced (Figure 5B). *BRD4* expression in lung tissue of rats was reduced after elevating miR-29a-3p (Figure 5C).

Downregulated miR-29a-3p or Upregulated *BRD4* Reverses the Function of *MORF4L1* Repression on PF

Concurrently with the combined intervention of PDN and CTX, we administered sh-*MORF4L1*+ miR-29a-3p antagomir, sh-*MORF4L1*+ antagomir NC, sh-*MORF4L1*+ oe-*BRD4*, and sh-*MORF4L1*+ oe-NC in rats, respectively. The successful injection was verified by RT-qPCR or Western blot (Figures 6A and 7A). After downregulating miR-29a-3p or upregulating *BRD4*, the effects of downregulating *MORF4L1* on PF were reversed (Figures 6B to 6G and 7B to 7G), further demonstrating that PDN combined with CTX ameliorated PF via the *MORF4L1*/miR-29a-3p/*BRD4* axis.

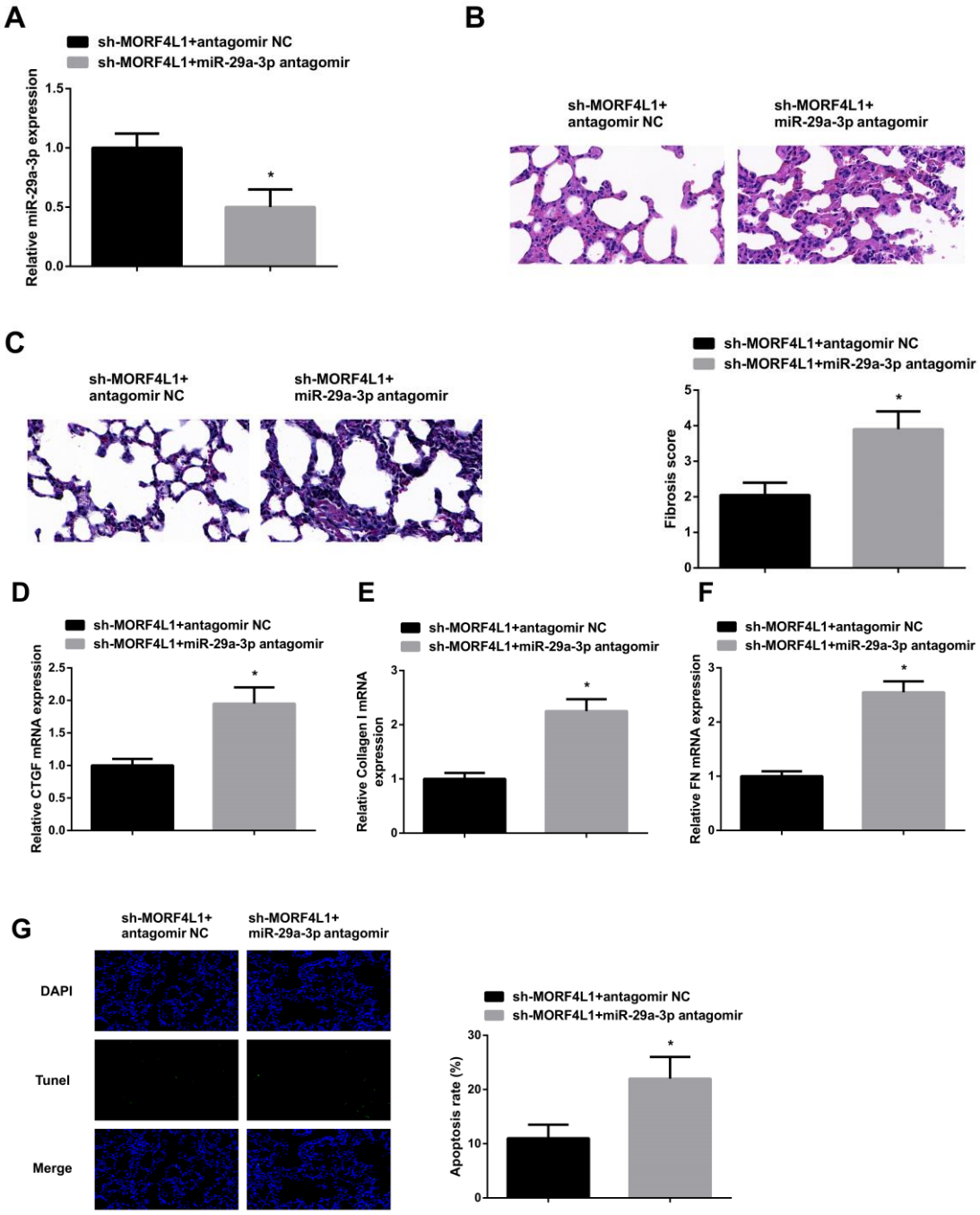

Figure 6. Downregulated miR-29a-3p reverses the function of repressive mortality factor 4 like 1 (*MORF4L1)* on PF
A. miR-29a-3p detected via real-time quantitative polymerase chain reaction (RT-qPCR); B. hematoxylin and eosin (HE) staining (400×) observed pathological condition of lung tissues, and the results showed that downregulation of miR-29a-3p weakened the inhibitory effect of downregulation *MORF4L1* on inflammatory cell infiltration; C. Masson staining (400×) observed pathological condition of lung tissues, and the results showed that downregulation of miR-29a-3p weakened the inhibitory effect of downregulation of *MORF4L1* on collagen deposition; D,E,F. RT-qPCR detected fibrosis-related markers connective tissue growth factor (CTGF), Collagen I, and fibronectin (FN) and found that downregulating miR-29a-3p attenuated the inhibitory effect of downregulating *MORF4L1* on the expression of fibrosis-related markers; G. terminal deoxynucleotidyl transferase dUTP nick end labeling (TUNEL) staining (400×) detected apoptosis of lung tissue cells and found that downregulating miR-29a-3p weakened the inhibitory effect of downregulating *MORF4L1* on lung cell apoptosis; The values were represented as mean±SD, n=6, * $p<0.05$ vs short hairpin (sh)-*MORF4L1* + antagonist to microRNA (antagomir) NC.

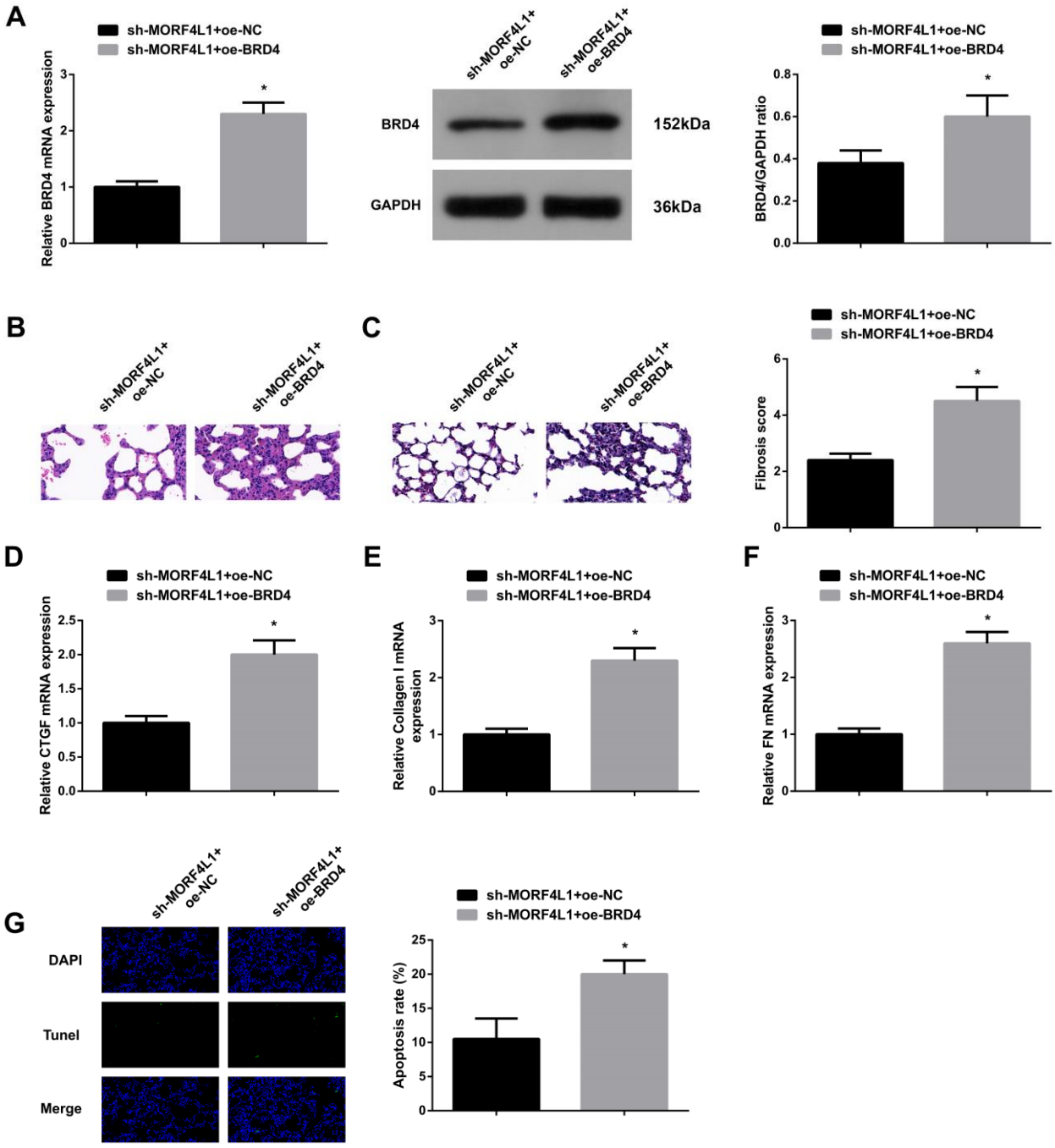

Figure 7. Elevated bromodomain-containing protein 4 (*BRD4)* reverses the influence of reduced *MORF4L1* on PF

A. *BRD4* detected by real-time quantitative polymerase chain reaction (RT-qPCR) and Western Blot; B. hematoxylin and eosin (HE) staining (400×) observed pathological condition of lung tissues, and the results showed that upregulation of *BRD4* weakened the inhibitory effect of downregulation of mortality factor 4 like 1 (*MORF4L1)* on inflammatory cell infiltration; C. Masson staining (400×) observed pathological condition of lung tissues, and the results showed that upregulation of *BRD4* weakened the inhibitory effect of downregulation of *MORF4L1* on collagen deposition; D,E,F. RT-qPCR detected fibrosis-related markers connective tissue growth factor (CTGF), collagen I, and fibronectin (FN) and found that upregulation of *BRD4* attenuated the inhibitory effect of downregulation of *MORF4L1* on the expression of fibrosis-related markers; G. terminal deoxynucleotidyl transferase dUTP nick end labeling (TUNEL) staining (400×) detected apoptosis of lung tissue cells and found that upregulation of *BRD4* weakened the inhibitory effect of downregulation of *MORF4L1* on lung cell apoptosis; The values were represented as mean±SD, n=6, * p<0.05 vs short hairpin (sh)-*MORF4L1* + overexpression (oe)-NC.

DISCUSSION

The primary objectives of this study were to assess the therapeutic impact of the combination of PDN and CTX, investigate its potential application in the treatment of PF, and ascertain its potential downstream regulatory mechanisms. The dosages of PDN (5 mg/kg) and CTX (15 mg/kg) employed in this investigation were estimated based on the dosages typically prescribed for patients with IPF.[15]

The rat model of PF was established by intratracheal injection of BLM, and expression of fibrosis-associated markers (CTGF, collagen I, and FN) was reduced in the PDN, CTX, or combined intervention groups. In addition, inflammatory cell infiltration and collagen deposition were significantly reduced, and the pathological condition was improved in PF rats in the PDN, CTX, or combined intervention groups. These findings align with previously suggested mechanisms and research on the effectiveness of PDN and CTX,[38-42] providing further evidence that PDN or CTX can alleviate PF.

PDN possesses anti-inflammatory and anti-allergic properties, inhibiting the proliferation of connective tissue and the synthesis and release of histamine and other harmful substances. Additionally, it reduces the permeability of cell membranes and capillary walls, thereby suppressing inflammatory exudation.[43,44] CTX is a common anticancer and immunosuppressive drug.[45,46] At present, 2 regimens for the treatment of PF are PDN combined with azathioprine or CTX.[13-15] However, the underlying mechanism of PDN combined with CTX in PF is unclear. This study is the first to demonstrate that PDN combined with CTX improves PF by regulating the *MORF4L1*/miR-29a-3p/*BRD4* axis.

circRNA molecules exhibit a closed-loop structure that remains unaffected by RNA exonucleases, rendering them highly stable and resistant to degradation. Functionally, circRNA molecules are enriched in miR binding sites and function as miR sponges within cells, thereby mitigating miR-mediated repression of target genes and enhancing the expression of target genes. This regulatory mechanism is commonly referred to as the competitive endogenous RNA (ceRNA) network.[47-49] circRNA exerts its influence on diseases through its interaction with miR.[50-52] According to a recent study, it has been established that the presence of circRNA *MORF4L1* in pneumonia promotes the process of apoptosis in epithelial cells.[25] In this study, it was confirmed that circRNA *MORF4L1* is upregulated in rats with PF. Additionally, it was observed that treatment with PDN or CTX can inhibit the expression of circRNA *MORF4L1*, leading to a decrease in levels of fibrosis-related proteins such as CTGF, collagen I, and FN, as well as apoptosis. Consequently, this effectively alleviates the symptoms of PF. In summary, the downregulation of *MORF4L1* can enhance the therapeutic effect of PDN or CTX on PF.

miRs, which are small non-coding RNAs, regulate mRNA expression by selectively targeting the 3′UTR of mRNA.[53-55] In this study, the expression of miR-29a-3p, a downstream miR of circRNA *MORF4L1*, was found to be suppressed in rats with PF. Elevating miR-29a-3p was observed to reduce the levels of fibrosis-associated proteins CTGF, collagen I, and FN, as well as apoptosis, thereby enhancing the therapeutic effects of PDN or CTX on PF. Additionally, it was discovered that *BRD4*, a downstream target of miR-29a-3p, is upregulated in PF, and this upregulation of *BRD4* can counteract the effects of the downregulation of circRNA *MORF4L1* on PF. A report has demonstrated that miR-29a-3p can inhibit the activation of lung fibroblasts.[31] Elevation of *BRD4* is detected in PF, and repression of *BRD4* can mitigate PF.[33,34] This is coincident with our experimental results.

However, this study has several limitations. Firstly, it solely focused on verifying the therapeutic effect of PDN combined with CTX on PF through in vivo animal experiments, without conducting any in vitro cell experiments. In order to further validate our findings, it is imperative to establish an in vitro PF model in future research. Secondly, the current study only examined the expression of circRNA *MORF4L1*/miR-29a-3p/*BRD4* in animal subjects, thus the generalizability of the research results to clinical settings is limited. Therefore, it is necessary to analyze the expression of circRNA *MORF4L1*/miR-29a-3p/*BRD4* in clinical cases of PF in future investigations.

Taken together, PDN with CTX mitigates PF through circRNA *MORF4L1*/miR-29a-3p/*BRD4* axis. The regulatory axis involving circRNA *MORF4L1*/miR-29a-3p/*BRD4* could potentially exert a significant influence on the pathogenesis and progression of PF. Furthermore, the findings of this investigation offer novel prospects for identifying therapeutic targets and devising strategies for the clinical management of PF.

STATEMENT OF ETHICS

The present study was approved by the Animal experiments were approved by Yueyang Hospital of Integrated Traditional Chinese and Western Medicine Animal Experimental Ethics Committee. And all procedures complied with the National Institutes of Health Guide for the Use of Laboratory Animals.

FUNDING

Supported by Funding of Yueyang Hospital of Integrated Traditional Chinese and Western Medicine, Shanghai University of Traditional Chinese Medicine (2019YYZ06).

CONFLICT OF INTEREST

The authors declare no conflicts of interest.

ACKNOWLEDGEMENTS

Not applicable.

REFERENCES

1. Rangarajan S, Bone NB, Zmijewska AA, Jiang S, Park DW, Bernard K, et al. Metformin reverses established lung fibrosis in a bleomycin model [published correction appears in Nat Med. 2018;24(8):1121-7.
2. Selman M, Pardo A, Kaminski N. Idiopathic pulmonary fibrosis: aberrant recapitulation of developmental programs? PLoS Med. 2008;5(3):e62.
3. Cao Z, Lis R, Ginsberg M, Chavez D, Shido K, Rabbany SY, et al. Targeting of the pulmonary capillary vascular niche promotes lung alveolar repair and ameliorates fibrosis. Nat Med. 2016;22(2):154-62.
4. Hofmann P, Sommer J, Theodorou K, Kirchhof L, Fischer A, Li Y, Perisic L, et al. Long non-coding RNA H19 regulates endothelial cell aging via inhibition of STAT3 signalling. Cardiovasc Res. 2019;115(1):230-42.
5. Inchingolo R, Varone F, Sgalla G, Richeldi L. Existing and emerging biomarkers for disease progression in idiopathic pulmonary fibrosis. Expert Rev Respir Med. 2019;13(1):39-51.
6. Liang H, Gu Y, Li T, Zhang Y, Huangfu L, Hu M, et al. Integrated analyses identify the involvement of microRNA-26a in epithelial-mesenchymal transition during idiopathic pulmonary fibrosis. Cell Death Dis. 2014;5(5):e1238.
7. Kulkarni T, O'Reilly P, Antony VB, Gaggar A, Thannickal VJ. Matrix Remodeling in Pulmonary Fibrosis and Emphysema. Am J Resp Cell Mol Biol. 2016;54(6):751-60.
8. Spagnolo P, Sverzellati N, Rossi G, Cavazza A, Tzouvelekis A, Crestani B, et al. Idiopathic pulmonary fibrosis: an update. Ann Med. 2015;47(1):15-27.
9. Chanda D, Otoupalova E, Smith SR, Volckaert T, De Langhe SP, Thannickal VJ. Developmental pathways in the pathogenesis of lung fibrosis. Mol Aspects Med. 2019;65(5):56-69.
10. Mora AL, Rojas M, Pardo A, Selman M. Emerging therapies for idiopathic pulmonary fibrosis, a progressive age-related disease. Nature reviews. Drug Discovery. 2017;16(11):755-72.
11. Barratt SL, Creamer A, Hayton C, Chaudhuri N. Idiopathic Pulmonary Fibrosis (IPF): An Overview. J Clin Med. 2018;7(8).
12. Taniguchi H, Ebina M, Kondoh Y, Ogura T, Azuma A, Suga M, et al. Pirfenidone in idiopathic pulmonary fibrosis. Europ Rsp J. 2010;35(4):821-9.
14. Oku H, Shimizu T, Kawabata T, Nagira M, Hikita I, Ueyama A, et al. Antifibrotic action of pirfenidone and prednisolone: different effects on pulmonary cytokines and growth factors in bleomycin-induced murine pulmonary fibrosis. Eur J Pharmacol. 2008;590(1):400-8.
15. Fiorucci E, Lucantoni G, Paone G, Zotti M, Li BE, Serpilli M, et al. Colchicine, cyclophosphamide and prednisone in the treatment of mild-moderate idiopathic pulmonary fibrosis: comparison of three currently available therapeutic regimens. Eur Rev Med Pharmacol Sci. 2008;12(2):105-11.
16. Chen L. The biogenesis and emerging roles of circular RNAs. Nature reviews. Mol Cell Biol. 2016;17(4):205-11.
17. Memczak S, Jens M, Elefsinioti A, Torti F, Krueger J, Rybak A, et al. Circular RNAs are a large class of animal RNAs with regulatory potency. Nature. 2013;495(7441):333-8.
18. Holdt LM, Stahringer A, Sass K, Pichler G, Kulak NA, Wilfert W, et al. Circular non-coding RNA ANRIL modulates ribosomal RNA maturation and atherosclerosis in humans. Nat Comm. 2016;7(1):12429.
19. Hu W, Han Q, Zhao L, Wang L. Circular RNA circRNA_15698 aggravates the extracellular matrix of diabetic nephropathy mesangial cells via miR-185/TGF-β1. J Cell Physiol. 2019;34(2):1469-76.
20. Kristensen LS, Hansen TB, Venø MT, Kjems J. Circular RNAs in cancer: opportunities and challenges in the field. Oncogene. 2018;37(5):555-65.
21. Hansen TB, Jensen TI, Clausen BH, Bramsen JB, Finsen B, Damgaard CK, et al. Natural RNA circles function as efficient microRNA sponges. Nature. 2013;495(7441):384-8.
22. Andrés-León E, Núñez-Torres R, Rojas AM. Rojas, miARma-Seq: a comprehensive tool for miRNA, mRNA and circRNA analysis. Sci Rep. 2016;6(5):25749.
23. Rong D, Sun H, Li Z, Liu S, Dong C, Fu K, Tang W, et al. An emerging function of circRNA-miRNAs-mRNA axis in human diseases. Oncotarget, 2017;8(42):73271-81.

24. Xiong DD, Dang YW, Lin P, Wen DY, He RQ, Luo DZ, et al. A circRNA-miRNA-mRNA network identification for exploring underlying pathogenesis and therapy strategy of hepatocellular carcinoma. J Transl Med. 2018;16(1):220.
25. Zou C, Li J, Xiong S, Chen Y, Wu Q, Li X, Weathington NM, et al. Mortality factor 4 like 1 protein mediates epithelial cell death in a mouse model of pneumonia. Sci Transl Med. 2015;7(311):311ra171.
26. Wu Q, Han L, Gui W, Wang F, Yan W, Jiang H. MiR-503 suppresses fibroblast activation and myofibroblast differentiation by targeting VEGFA and FGFR1 in silica-induced pulmonary fibrosis. J Cell Mol Med. 2020;24(24):14339-48.
27. Zhang J. The effects of miR-27a-3p-mediated Smurf2 on bleomycin A5-induced pulmonary fibrosis in rats. Cell Mol Biol. 2020;66(3):79-84.
28. Bai J, Deng J, Han Z, Cui Y, He R, Gu Y, Zhang Q. CircRNA_0026344 via exosomal miR-21 regulation of Smad7 is involved in aberrant cross-talk of epithelium-fibroblasts during cigarette smoke-induced pulmonary fibrosis. Toxicol Lett. 2021;347(12):58-66.
29. Cushing L. miR-29 is a major regulator of genes associated with pulmonary fibrosis. Am J Respir Cell Mol Biol. 2011;45(2):287-94.
30. van Rooij E, Sutherland LB, Thatcher JE, DiMaio JM, Naseem RH, Marshall WS, et al. Dysregulation of microRNAs after myocardial infarction reveals a role of miR-29 in cardiac fibrosis. Proc Natl Acad Sci U S A. 2008;105(35):13027-32.
31. Luo Y, Dong HY, Zhang B, Feng Z, Liu Y, Gao YQ, et al. miR-29a-3p attenuates hypoxic pulmonary hypertension by inhibiting pulmonary adventitial fibroblast activation. Hypertension. 2015;65(2):414-20.
32. Li P, Hao X, Liu J, Zhang Q, Liang Z, Li X, et al. miR-29a-3p Regulates Autophagy by Targeting Akt3-Mediated mTOR in SiO2-Induced Lung Fibrosis. Int J Mol Sci. 2023;24(14):11440.
33. Tang X, Peng R, Phillips JE, Deguzman J, Ren Y, Apparsundaram S, et al. Assessment of Brd4 inhibition in idiopathic pulmonary fibrosis lung fibroblasts and in vivo models of lung fibrosis. Am J Pathol. 2013;183(2):470-9.
34. Sanders YY, Lyv X, Zhou QJ, Xiang Z, Stanford D, Bodduluri S, et al. Brd4-p300 inhibition downregulates Nox4 and accelerates lung fibrosis resolution in aged mice. JCI insight. 2020;5(14).
35. Chen Y, Zhang Q, Zhou Y, Yang Z, Tan M. Inhibition of miR-182-5p attenuates pulmonary fibrosis via TGF-β/Smad pathway. Hum Exp Toxicol. 2020;39(5):683-95.
36. Wang Y., et al., Hepatic NPC1L1 overexpression attenuates alcoholic autophagy in mice. Mol Med Rep. 2019;20(4):3224-32.
37. Zhou J. Effect of fecal microbiota transplantation on experimental colitis in mice. Exp Ther Med. 2019;17(4):2581-6.
38. Aso S. Systemic glucocorticoids plus cyclophosphamide for acute exacerbation of idiopathic pulmonary fibrosis: a retrospective nationwide study. Sarcoidosis Vasc Diffuse Lung Dis. 2019;36(2):116-23.
39. Naccache JM, Montil M, Cadranel J, Cachanado M, Cottin V, Crestani B, et al. Study protocol: exploring the efficacy of cyclophosphamide added to corticosteroids for treating acute exacerbation of idiopathic pulmonary fibrosis; a randomized double-blind, placebo-controlled, multi-center phase III trial (EXAFIP). BMC pulmonary medicine, 2019;19(1):75-9.
40. Hozumi, H. Efficacy of corticosteroid and intravenous cyclophosphamide in acute exacerbation of idiopathic pulmonary fibrosis: A propensity score-matched analysis. Respirology. 2019;24(8):792-8.
41. Yu W, Guo F, Song X. Song, Effects and mechanisms of pirfenidone, prednisone and acetylcysteine on pulmonary fibrosis in rat idiopathic pulmonary fibrosis models. Pharm Biol. 2017;55(1):450-5.
42. Gothe F, Schmautz A, Häusler K, Tran NB, Kappler M, Griese M. Treating Allergic Bronchopulmonary Aspergillosis with Short-Term Prednisone and Itraconazole in Cystic Fibrosis. J Allergy Clin Immunol Pract. 2020;8(8):2608-2614.e3.
43. Zhang H. Prednisone Ameliorates Atrial Inflammation and Fibrosis in Atrial Tachypacing Dogs. Int Heart J. 2022;63(2):347-55.
44. Gao H. Combined therapy of prednisone and mTOR inhibitor sirolimus for treating retroperitoneal fibrosis [published correction appears in Ann Rheum Dis. Ann Rheum Dis. 2023;82(5):688-97.
45. Ahlmann M, Hempel G. The effect of cyclophosphamide on the immune system: implications for clinical cancer therapy. Cancer Chemother Pharmacol. 2016;78(4):661-71.
46. Teles KA, Medeiros-Souza P, Lima FAC, Araújo BG, Lima RAC. Cyclophosphamide administration routine in autoimmune rheumatic diseases: a review. Rev Bras Reumatol Engl Ed. 2017;57(6):596-604.
47. Liu H, Wang X, Wang ZY, Li L. Circ_0080425 inhibits cell proliferation and fibrosis in diabetic nephropathy via sponging miR-24-3p and targeting fibroblast growth factor 11. J Cell Physiol. 2020,235(5):4520-9.

48. Li G, Qin Y, Qin S, Zhou X, Zhao W, Zhang D. Circ_WBSCR17 aggravates inflammatory responses and fibrosis by targeting miR-185-5p/SOX6 regulatory axis in high glucose-induced human kidney tubular cells. Life Sci. 2020;259(14):18269.
49. Li S, Song F, Lei X, Li J, Li F, Tan H. hsa_circ_0004018 suppresses the progression of liver fibrosis through regulating the hsa-miR-660-3p/TEP1 axis. Aging. 2020;12(12):11517-29.
50. Ji D, Chen GF, Wang JC, Ji SH, Wu XW, Lu XJ, et al. Hsa_circ_0070963 inhibits liver fibrosis via regulation of miR-223-3p and LEMD3. Aging, 2020;12(2):1643-55.
51. Wang W, Feng J, Zhou H, Li Q. Circ_0123996 promotes cell proliferation and fibrosisin mouse mesangial cells through sponging miR-149-5p and inducing Bach1 expression. Gene. 2020;761(5):144971.
53. Ai K, Zhu X, Kang Y, Li H, Zhang L. miR-130a-3p inhibition protects against renal fibrosis in vitro via the TGF-β1/Smad pathway by targeting SnoN. Exp Mol Pathol. 2020;112(23):104358.
54. Cheng L, Tu C, Min Y, He D, Wan S, Xiong F. MiR-194 targets Runx1/Akt pathway to reduce renal fibrosis in mice with unilateral ureteral obstruction. Int Urol Nephrol. 2020;52(9):1801-8.
55. Xue Y, Fan X, Yang R, Jiao Y, Li Y. miR-29b-3p inhibits post-infarct cardiac fibrosis by targeting FOS. Biosci Rep. 2020;40(9).